Originally appeared in *Pyrotechnica XIV* (1992).

Computer Modeling of Aerial Shell Ballistics

by K.L. and B.J. Kosanke

ABSTRACT

If one has a reasonably accurate computer model, it is usually appropriate (cheaper and faster) to rely primarily on modeled results, supplemented with limited experimental results. The case of aerial shell ballistics is no exception. The mathematical basis for such a ballistics model is derived, and the simplifications and assumptions of the model are considered. The necessary input parameters are developed and some modeling results are presented. Finally, the use of the model is demonstrated by performing a series of calculations, including the effect of mortar tilt angle and wind speed.

Introduction

A knowledge of fireworks aerial shell ballistics is of more than academic interest. It is the basis for answering several important questions dealing with fireworks displays. For example: (1) What is the appropriate mortar tilt angle to use to compensate for a given wind condition? (2) Under a given set of conditions, where in the sky will properly performing aerial shells break? (3) In the event that a shell fails to break (is a dud), where will it fall to earth? (4) For shells properly breaking at a given altitude, where will the shell debris fall to earth? (5) For a specific time delay, provided by the time fuse, how near the apogee (highest point) will the shell be when it bursts? Answering questions such as these requires information about aerial shell ballistics. The needed information can come from guesses based on experience (generally unreliable), from specific field experiments (always expensive), or from ballistics calculations (generally reliable and always inexpensive). Thus the use of ballistics calculations, guided by practical experience and occasionally verified empirically, is the best choice for answering questions such as those posed above.

Following a general discussion of computer modeling, this paper presents a derivation of the equations used in the authors' computer modeling of aerial shell ballistics. The model is three-dimensional and includes the effects of mortar angle and wind conditions. Also presented is an empirical determination of the drag coefficient for spherical shells, information about tests of the computer model, and some results determined through its use.

Computer Modeling Analogy

Before computers were available, physicists solved problems analytically. They solved complex equations using high-level mathematics and obtained exact answers. The difficulty was that only the very simplest of problems could be solved in this way. For the more interesting and complex problems, simplifying assumptions and approximations had to be made. At best this resulted in only approximate answers; and, often, even after simplifying the problems they remained unsolvable.

Now that computers are available, the whole approach to problem solving has changed. Computers do not make it easier to get analytic (exact mathematical) solutions to complex problems, but they offer a level of "brute force" arithmetic that is simply astounding. Even the most inexpensive personal computers can perform more arithmetic calculations in a few hours than a physicist could in a lifetime. This has made it practical to use a much simpler (if also less elegant) approach to problem solving; that approach is termed modeling. While computer modeling is not an exact solution to a problem, it can yield results as close to the exact solution as necessary, provided enough computer time is used. In computer modeling there is always a trade-off between the time needed to produce an answer and the accuracy of that answer. The nature of this trade-off is illustrated in the following example.

Imagine that the problem to be solved is to determine the length of the curved line shown in Figure 1a, and the only tool available is a ruler. The easiest approach is simply to place the ruler from the start to the end and read the result (see

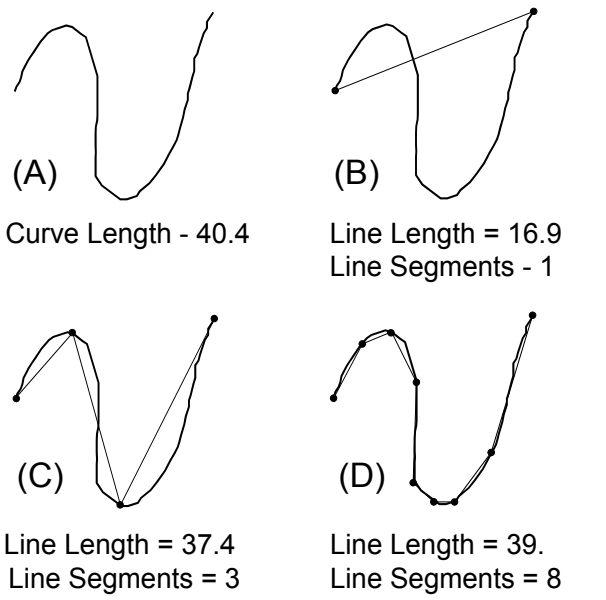

Figure 1. Determining the length of a curved line with a ruler.

Figure 1b). This is fast, but obviously seriously underestimates the length of the curved line. Suppose instead, that the ruler was laid along the line as shown in Figure 1c. In this case three measurements are taken and summed. This took longer but obviously produced a much better estimate of the length of the curved line. In Figure 1d this approach is carried further; here eight measurements are taken and summed. Again more time was taken, but now a good estimate of the length of the curved line has resulted. If it were only necessary to know the length to within a few percent, then this would be sufficient. If still greater accuracy is needed, all that would be required is to measure even more individual segments. Theoretically, no matter how much accuracy is needed, greater and greater numbers of line segments could be measured until their total yielded an answer with the required accuracy; the only limitation is the amount of time available for the measurements.

The above example illustrates how this same problem might be solved on a computer. Problems are broken into very many small steps and solved in a brute force fashion. It is not elegant, but it works, and it allows solutions to many problems that cannot be solved analytically.

When complex problems are solved using computers by dividing the problem into smaller and smaller parts, it is important to know when the individual parts are small enough. The above example also illustrates how this is done. Consider the change upon increasing from using one line segment to using three line segments. In this case the estimate of length increased considerably, about 120%. Now consider the change upon increasing from using three to eight line segments. This time the estimate of length only increased slightly, approximately 5%. In computer modeling, when calculated results change very little as the problem is broken into ever smaller parts, the modeled result is generally very close to the exact solution.

Computer Modeling of Aerial Shell Ballistics

Problems in classical mechanics, such as aerial shell ballistics, are well suited to computer modeling and excellent results can be attained. In general, this type of problem can be stated as: given the force laws operating, determine the acceleration of the object; from that and initial conditions for position and velocity determine its path. In a computer model of aerial shell ballistics this is accomplished as a repeating series of steps:

1) Start at the muzzle of the mortar with the shell having its initial (muzzle) velocity ($\boldsymbol{v}$).
2) Choose the small time interval (Δt) to be used.
3) Calculate the force ($\boldsymbol{F}$) acting on the shell at the start of the time interval.
4) Using Newton's Second Law of Motion ($\boldsymbol{F}=m\boldsymbol{a}$), calculate the acceleration ($\boldsymbol{a}$) of the shell during that time interval.
5) Calculate the change in velocity ($\Delta\boldsymbol{v} = \boldsymbol{a}\Delta t$), and the average velocity ($\bar{v} = \boldsymbol{v} + \frac{1}{2}\Delta\boldsymbol{v}$) of the shell.
6) Calculate the change in shell position ($\Delta\boldsymbol{r} = \bar{v}\,\Delta t$).
7) The velocity and position for the shell at the end of the time interval are $\boldsymbol{v} + \Delta\boldsymbol{v}$ and $\boldsymbol{r} + \Delta\boldsymbol{r}$, and the time is now $t + \Delta t$.
8) Unless the shell has returned to the ground, return to step 3 and continue the calculations using the new values from step 7.

Following this procedure the aerial shell is stepped along its trajectory until it returns to the ground. In the limit as Δt approaches zero, the modeled trajectory is exactly equal to the actual trajectory of the shell. Of course, this means there would be an infinite number of steps along the trajectory, which would require an infinite time to run on a computer. As a practical matter, when Δt is set to 0.01 second, the errors in the modeled results are vanishingly small in comparison to errors resulting from uncertainties in initial conditions such as muzzle velocity, wind speed and direction, mortar tilt and direction, air mass density, and the shell's drag coefficient.

In the above steps, two types of variables are used, scalars such as t (shown in normal typeface), and vectors such as $\boldsymbol{F}$, $\boldsymbol{a}$, $\boldsymbol{v}$, and $\boldsymbol{r}$ (shown in bold italic typeface). It is important to understand the difference between the two types of variables. Time (t) is a scalar because, while it has magnitude, it does not have a direction in three-dimensional space. Similarly, speed (v) is a scalar quantity because it is used without reference to direction. On the other hand, velocity ($\boldsymbol{v}$) is a vector because it has both magnitude and direction. (The concept of scalars and vectors is not an easy one to grasp. If the reader does not have experience with these, it may become clearer in the next section of this paper. If after completing this paper, the reader wishes more information about scalar and vector quantities and how they are used mathematically, a college physics text should be consulted.)

Derivation of the Computer Model Equations

Readers wishing to be spared the tedium of the derivation should skip to the next section. Before beginning the actual derivation of the computer model equations, it is first necessary to define some parameters and lay some additional groundwork.

A) The model uses Cartesian coordinates, with the mortar located at the origin, and the Z–direction corresponds to the height, see Figure 2A.

B) The placement of the mortar is defined by two angles, tilt (τ) and azimuth (α).

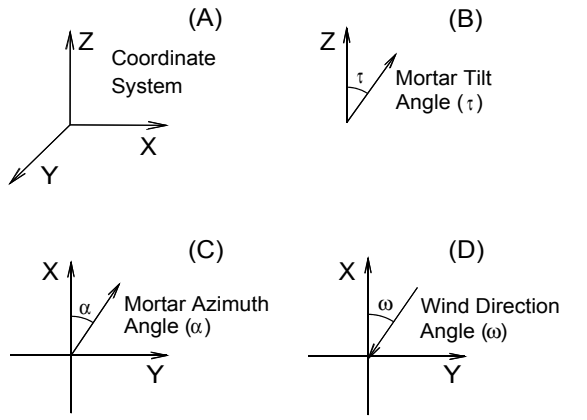

Figure 2. Coordinate system with mortar tilt angle (τ), mortar azimuth angle (α), and wind direction angle (ω) defined.

1) The tilt angle is measured in degrees from vertical (the Z–axis) i.e., $\tau = 0°$ corresponds to vertical mortar placement, see Figure 2B.

2) The azimuth is the mortar angle projected onto the X–Y plane, measured from the X–axis, with clockwise rotation corresponding to positive angles, see Figure 2C. For example, a mortar tilted in the X–direction has $\alpha = 0°$, and a mortar tilted in the Y–direction has $\alpha = 90°$.

C) It is assumed that the wind has no vertical component. Thus only one angle is needed for its direction. The wind direction (ω) is the direction of the origin of the wind, measured from the X–axis, with clockwise rotation corresponding to positive angles. For example, a wind coming from the X–direction has $\omega = 0°$, and a wind coming from the minus Y–direction has $\omega = 270°$.

D) The model uses metric units internally, but all input and output are converted to English units for convenience.

As the aerial shell emerges from the mortar, it is acted on by a net force ($\boldsymbol{F}_s$), which is the sum of two forces, gravity ($\boldsymbol{F}_g$) and the aerodynamic drag ($\boldsymbol{F}_d$):

$$\boldsymbol{F}_s = \boldsymbol{F}_g + \boldsymbol{F}_d. \qquad (1)$$

The gravitational force (or weight) is simply

$$\boldsymbol{F}_g = m\,\mathbf{g}, \qquad (2)$$

where m is the mass of the shell in kilograms, and **g** is the acceleration due to gravity (9.8 meters per second^2).

The magnitude of the aerodynamic drag force is[1,2]

$$F_d = \tfrac{1}{2} C_d \rho_m S v_a^2, \quad (3)$$

where C_d is the drag coefficient for the shell (a dimensionless constant which must be determined empirically), ρ_m s the mass density of air (1.28 kg/m^3 at sea level), S is the projected area of the shell, and v_a is the relative speed of the air past the shell.

Converting Equation 3 into vector notation

$$\boldsymbol{F}_d = \tfrac{1}{2} C_d \rho_m S \boldsymbol{u}_a v_a^2, \quad (4)$$

where $\boldsymbol{u}_a$ is the air velocity unit vector (which has the same direction as $\boldsymbol{v}_a$).

The air flowing past an aerial shell ($\boldsymbol{v}_a$), arises in part from the wind $\boldsymbol{W}$, but more significantly from the motion of the shell itself. The component of air velocity resulting from the shell's motion is equal in magnitude to the velocity of the shell $\boldsymbol{v}_s$ but opposite in direction. Thus,

$$\boldsymbol{v}_a = \boldsymbol{W} - \boldsymbol{v}_s. \quad (5)$$

By substitution of Equations 2 and 4 into Equation 1, the force acting on the aerial shell is

$$\boldsymbol{F}_s = m\,\mathbf{g} + \tfrac{1}{2} C_d \rho_m S \boldsymbol{u}_a v_a^2. \quad (6)$$

Using Newton's Second Law of Motion ($\boldsymbol{F} = m\boldsymbol{a}$), the resulting acceleration of the shell $\boldsymbol{a}_s$ is

$$\boldsymbol{a}_s = \mathbf{g} + K \boldsymbol{u}_a v_a^2, \quad (7)$$

where the constant K has been substituted for the quantity ($\tfrac{1}{2} C_d \rho_m$ S/m).

From general physics, $\Delta\boldsymbol{v} = \boldsymbol{a}\,\Delta t$, where $\Delta\boldsymbol{v}$ is the change in velocity produced by constant acceleration. Thus the change in shell velocity $\Delta\boldsymbol{v}_s$ occurring during the short time interval Δt is

$$\Delta\boldsymbol{v}_s = \mathbf{g}\,\Delta t + K \boldsymbol{u}_a v_a^2\,\Delta t. \quad (8)$$

For constant acceleration, the average shell velocity $\bar{v}_s$, during the time interval Δt, is simply

$$\bar{v}_s = \boldsymbol{v}_s + \tfrac{1}{2}\Delta\boldsymbol{v}_s, \quad (9)$$

where $\boldsymbol{v}_s$ is the shell velocity at the start of the time interval.

At the start of the first time interval, shell velocity $\boldsymbol{v}_s$ is the muzzle velocity. For all subsequent time intervals, the starting shell velocity is simply the starting shell velocity for the previous interval plus the change in shell velocity $\Delta\boldsymbol{v}_s$ (Equation 8) occurring during that previous time interval.

Again from general physics, $\Delta\boldsymbol{r} = \bar{v}\,\Delta t$, where $\Delta\boldsymbol{r}$ is the change in position. Thus, the change in shell position $\Delta\boldsymbol{r}_s$ occurring during the short time interval is

$$\Delta\boldsymbol{r}_s = \bar{v}_s\,\Delta t. \quad (10)$$

At the start of the first time interval, the shell position is at the mortar muzzle, which is the origin for the coordinate system. For all subsequent time intervals, starting shell position is simply the starting shell position for the previous interval plus the change in position $\Delta\boldsymbol{r}_s$ (Equation 10) occurring in the previous time interval.

The next (and most tedious) step in deriving the equations for the model is to resolve Equations 8 and 10, which contain vector quantities, into sets of three equations containing only scalar variables. In the coordinate system defined above, any of the vector quantities can be resolved into three component vectors, one along each axis. For example, the shell's vector velocity can be expressed as

$$\boldsymbol{v}_s = \boldsymbol{v}_{sx} + \boldsymbol{v}_{sy} + \boldsymbol{v}_{sz}. \quad (11)$$

Further, each of the three component vectors can be expressed as the product of its scalar magnitude and a unit vector $\boldsymbol{u}$ along the axis,

$$\boldsymbol{v}_s = v_{sx} \boldsymbol{u}_x + v_{sy} \boldsymbol{u}_y + v_{sz} \boldsymbol{u}_z. \quad (12)$$

At time zero, when the shell has just exited the mortar, its velocity will be the muzzle velocity. Using basic trigonometric relationships, the magnitudes of the three initial velocity components are:

$$v_{sz} = v_m \cos(\tau), \quad (13)$$

$$v_{sx} = v_m \sin(\tau) \cos(\alpha), \text{ and} \quad (14)$$

$$v_{sy} = v_m \sin(\tau) \sin(\alpha), \quad (15)$$

where v_m is the scalar muzzle velocity of the shell.

Using basic trigonometric relationships, and recalling that it is assumed that there is no Z–

component, the three components for the true wind W are:

$$W_z = 0, \quad (16)$$

$$W_x = -W \cos(\omega), \text{ and} \quad (17)$$

$$W_y = -W \sin(\omega), \quad (18)$$

where W is the scalar true wind velocity, and the minus sign converts the direction for the origin of the wind to the direction toward which the wind is blowing.

Thus using Equation 5 and the above equations, the magnitudes of the three components of the air velocity are:

$$v_{az} = -v_{sz}, \quad (19)$$

$$v_{ax} = [-W \cos(\omega)] - v_{sx}, \text{ and} \quad (20)$$

$$v_{ay} = [-W \sin(\omega)] - v_{sy}. \quad (21)$$

To calculate the change in shell velocity using Equation 8, the magnitude of the air velocity is also needed, which by combining its components, is:

$$v_a = [v_{ax}^2 + v_{ay}^2 + v_{az}^2]^{1/2}. \quad (22)$$

To resolve $\boldsymbol{u}_a$ into its components along the coordinate axes, it is necessary to determine its tilt angle σ and azimuth angle ß, see Figure 3. Using basic trigonometric relationships:

$$\sigma = \text{Cos}^{-1} (v_{az}/v_a), \text{ and} \quad (23)$$

$$ß = \text{Tan}^{-1} (v_{ay}/v_{ax}). \quad (24)$$

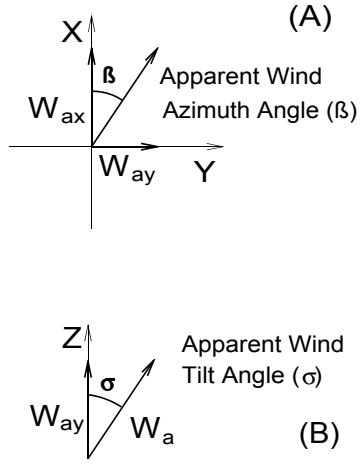

Figure 3. Apparent wind azimuth angle (β) and apparent wind tilt angle (σ) defined.

Then, again using basic trigonometric relationships, the magnitudes of the projections of $\boldsymbol{u}_a$ are:

$$u_{ax} = \text{Sin}(\sigma) \text{ Cos}(ß), \quad (25)$$

$$u_{ay} = \text{Sin}(\sigma) \text{ Sin}(ß), \text{ and} \quad (26)$$

$$u_{az} = \text{Cos}(\sigma). \quad (27)$$

The set of model equations for velocity change during the time interval Δt, result from substitution of the above equations into Equation 8 and recalling that the only non-zero component of **g** is $\mathbf{g}_z$ which is in the minus Z–direction:

$$\Delta v_{sx} = K v_a^2 \text{ Sin}(\sigma) \text{ Cos}(ß) \Delta t, \quad (28)$$

$$\Delta v_{sy} = K v_a^2 \text{ Sin}(\sigma) \text{ Sin}(ß) \Delta t, \text{ and} \quad (29)$$

$$\Delta v_{sz} = -\mathbf{g}_z \Delta t + K v_a^2 \text{ Cos}(\sigma) \Delta t. \quad (30)$$

The set of model equations for position change during the same time interval is just Equation 10 resolved into its components:

$$\Delta r_{sx} = (v_{sx} + ½ \Delta v_{sx}) \Delta t, \quad (31)$$

$$\Delta r_{sy} = (v_{sy} + ½ \Delta v_{sy}) \Delta t, \text{ and} \quad (32)$$

$$\Delta r_{sz} = (v_{sz} + ½ \Delta v_{sz}) \Delta t. \quad (33)$$

In Equations 19 through 21 and 31 through 33, the v_s terms are the shell velocity components at the start of the time interval. During the very first time interval, these values are calculated using the muzzle velocity and Equations 13 through 15. Subsequently, they are just the velocity components after the previous time interval.

The authors have not included a copy of their computer program in this paper because it is considered proprietary. However, using Equations 28 through 33 and following the procedural steps for the model listed in the previous section, it is a relatively simple matter to write a computer program to implement the model.

Model Simplifications and Assumptions

As aerial shells are propelled from a mortar, they almost always begin to tumble (spin), sometimes a little, sometimes a lot. The magnitude of the tumbling is impossible to predict; also unpredictable is the orientation of the spinning. The effect of shell spinning is similar to a curve-ball pitch in baseball; it will deviate from its ballisti-

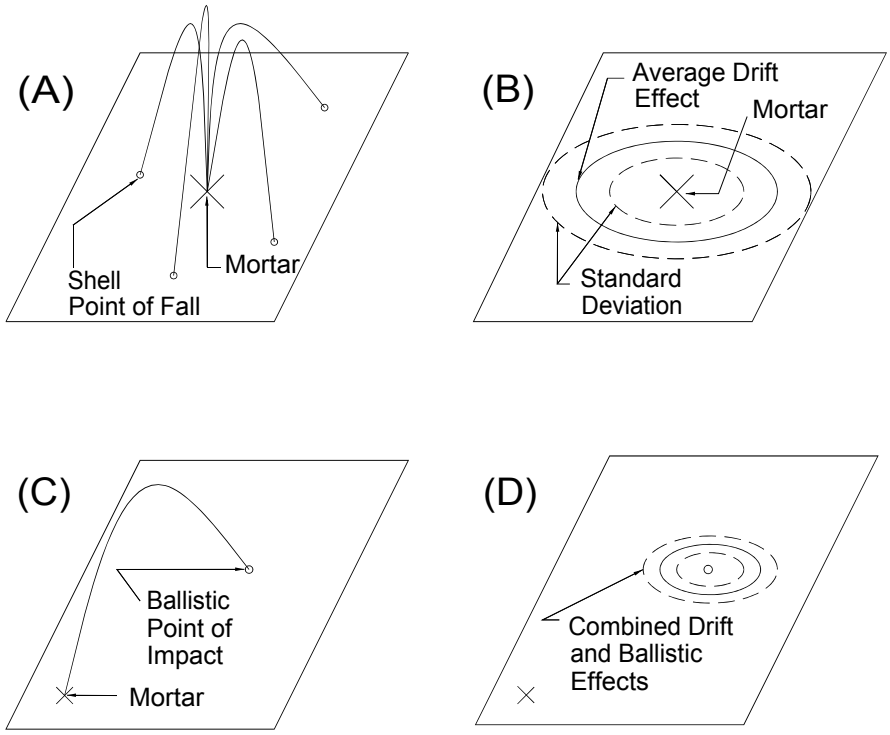

Figure 4. Inclusion of drift effects into ballistic results from a model.

cally predicted path. In addition, there are other factors that also contribute to an aerial shell "drifting" away from its ballistically predicted path. Because the magnitude and orientation of these "drift effects" cannot be known in advance, it is not possible to include the drift effect into the model without first determining the probability of various drifts occurring and then using so-called Monte Carlo techniques in the computer model. (A discussion of Monte Carlo modeling techniques is beyond the scope of this article. Suffice it to say that: it is a method by which effects that are only knowable on a statistical level can be incorporated into a computer model; a factor of about 100 more computer time is required for the calculations; and those modeled results are not absolute but only statistical in nature. Readers wishing more information on Monte Carlo techniques are referred to a university level text on numerical analysis.) Fortunately, there is an easier and faster way to include drift effects into computer modeled results. Many physics problems, which are difficult to solve, can be made easier by separating the problem into parts, finding answers for each part, and then combining the parts to get the overall solution. This method was attempted by the authors.

The method by which drift effects are included in the ballistic results from the model is illustrated in Figure 4. First, (Figure 4A) a series of dud aerial shells of a given shape and size are fired into the air. The shells were rendered duds by having water injected into their time fuses. The locations at which the shells fall to the ground are recorded. From this information, statistical parameters (the average distance of the points-of-fall from the mortar and the standard deviation about the average) are calculated (Figure 4B). Next, (Figure 4C) the ballistics model is used to predict the trajectory of a non-drifting shell. Finally, (Figure 4D) drift effects are added to the ballistic result, predicting the center of probable points-of-fall, how far from the center an average shell will fall, and the statistical distribution of points-of-fall about the average.

When complex problems can be separated into parts, solved separately, and then successfully recombined to give accurate results, they are said to be linear. While it is unlikely that the drifting aerial shell problem is absolutely linear, tests such as one described later in this article, indicate that the effects of any non-linearity in this problem are small enough to be safely ignored.

Another simplifying assumption (presently being made) is that the aerodynamic drag coefficient (C_d) for the aerial shell is constant, independent of air velocity. This is certainly not true. At the high speed of a typical aerial shell as it leaves the mortar, the airflow around the shell will be turbulent. Whereas, near the apex of its trajectory, when the speed of the shell is low, the airflow will be nearly laminar. The drag coefficients for these two cases are significantly different. In the present model, an average value for the drag coefficient, or what might be called an effective drag coefficient, is used. This works well, providing the conditions being modeled and those operating when the effective drag coefficient was determined are similar regarding the magnitude of air velocity. Fortunately, such close similarity exists for most of the situations of interest in aerial shell ballistics modeling. (In the event that cases for study required a velocity-dependent drag coefficient that upgrade to the model can easily be made.)

Finally, the model assumes the true wind is constant, independent of height above the ground and unchanging over the time-of-flight of the aerial shell being modeled. Rarely is this ever the case, and it would be a simple matter to include such effects into the model. However, this was not done for two reasons: wind effects on an intact aerial shell are relatively small in comparison with other effects such as mortar angle; and, more importantly, one essentially never has even crude information regarding wind conditions aloft.

For this model, the above simplifying assumptions will occasionally introduce errors into the results. However, uncertainties in other parameters, such as muzzle velocity for an individual shell can introduce significantly larger errors. Thus the simplifying assumptions are appropriate.

Determination of Aerial Shell Drift Effects

The determination of drift effects of aerial shells is underway. Drift effects for spherical shells from three-inch to ten-inch have been determined.[3] For spherical shells fired from vertical mortars with no wind, the drift effect would cause them to fall at an average of 32 feet away from the mortar for each inch of shell size. Thus, on average, a three-inch dud shell would fall approximately 100 feet from the point-of-fall predicted for a non-drifting shell. Finally, the coefficient of variation of the distribution of the points-of-fall averages 42% for fall points below the mean and 97% for fall points above the mean.[34] (Note: the coefficient of variation is standard deviation expressed as a percentage of the mean.) As further studies are completed, their results will be reported.

Determination of Aerial Shell Drag Coefficients

The drag coefficient for spherical aerial shells was determined empirically using T. Shimizu's published shell performance data in.[35] Using Shimizu's values for muzzle velocity, mass, and projected area, the drag coefficient of the model was adjusted until there was agreement with Shimizu's measurements of shell apogee and then flight time to impact. In this way 15 drag coefficients were determined. These results are plotted in Figure 5. (Note that Japanese shell sizes are measured in "suns," with 1 sun = 1.19 inches, and is the reason the shell sizes are not integer inches. Also, it should be noted that Shimizu occasionally reported two sets of results for the same size shell; this corresponds to normal and low mass shells.) There is a fair amount of scatter in the drag coefficient data in Figure 5. This makes it difficult to determine whether the drag coefficients for spherical shells are a function of shell size. When a linear least squares fit was attempted with the data, the correlation coefficient was –0.69, suggesting only a moderate degree of correlation between drag coefficient and shell size. (A full discussion of correlation coefficients is beyond the scope of this article. Suffice it to say that correlation coef-

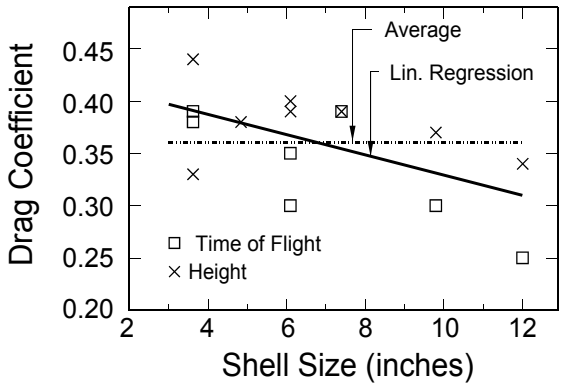

Figure 5. Drag coefficients for spherical aerial shells.

ficients range from –1 to 0 to +1 with: –1 indicating a perfect inverse correlation, 0 indicating absolutely no correlation, +1 indicating a perfect direct correlation, and values between suggesting correlations with varying degrees of certainty.) Table 1 lists drag coefficients as a function of shell size, as determined using the slope and intercept from the least squares fit.

Table 1. Spherical Aerial Shell Drag Coefficient as a Function of Shell Size.

Aerial Shell Size (inches)	Drag Coefficient
3	0.397
4	0.387
5	0.377
6	0.368
8	0.348
10	0.329
12	0.310
Average of all Data Points = 0.359	

As a check on the appropriateness of these drag coefficients, they were used in an attempt to reproduce Shimizu's measured times to apogee and heights of apogee. Note that this should work well because this is the same data that was originally used in determining the drag coefficients. It was found that the average deviations between modeled and measured times to apogee and heights of apogee were 0.1 second and 39 feet, respectively. As a point of reference, when Shimizu's outer ballistics equations (Shimizu, 1985, Section 12.3) were used with the same data, the average deviations between calculated and measured times to apogee and heights of apogee were 0.6 seconds and 48 feet, respectively. Thus, at least with the Shimizu data, the above drag coefficients work well.

Because the degree of correlation between shell size and drag coefficient was not particularly good, it was decided to investigate whether the use of a single average drag coefficient would result in a significant increase in average deviations reported above. When a coefficient of 0.36 was used, the average deviations between modeled and measured times to apogee and heights of apogee were 0.3 second and 34 feet, respectively. This corresponds to a moderate worsening of average deviation in times to apogee and a slight improvement in the deviation of heights of apogee. While these results are not quite as good as when shell size dependent drag coefficients were used, they are not so bad as to reject the use of an average drag coefficient independent of spherical shell size. The limited results given herein as examples were produced using 0.36 as the drag coefficient.

Drag coefficients for cylindrical shells could be determined in much the same way as above, providing one has access to similar empirical data. Unfortunately, the authors are not aware of any such data. The situation is further complicated because the average drag coefficient for cylindrical shells will be a function of the shell's aspect ratio (ratio of the shell's length to diameter), and shell aspect ratios vary significantly between different types of shells. At the time of submission of this article, the authors have just started work to determine drag coefficients for cylindrical shells.

Determination of Optimum Time Interval for Model Iterations

In the computer modeling analogy at the beginning of this article, it was demonstrated that as the problem is broken into ever-smaller steps (iterations), the modeled result approaches the true (analytic) solution to the problem. It was also demonstrated that the law of diminishing returns plays an important role, and that there soon comes a point where the gains resulting from ever smaller steps becomes insignificant, especially when considering the added time necessary to achieve those slight improvements. Thus, one way to establish when the problem has been broken into small enough steps is to observe the results as one uses ever-smaller steps.

In this computer model, the iteration interval (step size) is a time interval. To establish the optimum time interval the following problem (from Shimizu's data) was considered:

- Shell Muzzle Velocity = 390 feet/second,
- Shell Size = 6.85 inches,
- Shell Weight = 4.65 pounds,
- Mortar Tilt Angle = 0°,
- Wind Speed = 0 miles/hour,
- Drag Coefficient = 0.36, and
- Elevation above Sea-Level ≈ 0 feet.

Table 2 lists the results of a series of modeled results using ever-shorter time intervals.

Table 2. Modeled Results for Various Iteration Time Intervals.

Time Interval (seconds)	Time to Apogee (seconds)	Apogee Height (feet)	Time to Impact (seconds)
1.0	5.8	775	13.4
0.1	6.71	949	15.43
0.01	6.78	965	15.60
0.001	6.79	966	15.62

Only an insignificant change resulted from reducing the time interval by the factor of ten from 0.01 to 0.001 second. Using 0.001 second as the time interval, the computer program required nearly 27 minutes to run, whereas when the time interval was 0.01 second it required only a little more than 2.5 minutes. (Note that these times are for a 286 CPU, IBM-compatible computer without a math co-processor.) Obviously time intervals of 0.01 second are optimum in terms of run time and accuracy. In the modeling results reported in the remainder of this article, 0.01 second was used as the time interval.

Model Testing

In those imaginary cases when aerodynamic drag is zero, the problem of aerial shell ballistics becomes so simple that it is possible to calculate exact mathematical solutions. Thus the first test of the model was to verify that it successfully reproduced those analytic results. For example, with $C_d = 0$, for any projectile (independent of mass or projected area) fired vertically into the air, from general physics it is known that:

$$t_a = v_m / \mathbf{g}, \quad (34)$$

where t_a is the time to apogee; v_m is muzzle velocity, and **g** is the acceleration due to gravity.

$$Z_a = v_m^{\,2} / 2\,\mathbf{g}, \quad (35)$$

where Z_a is the height of apogee;

$$t_i = 2\,t_a, \quad (36)$$

where t_i is the time to impact; and

$$v_i = -v_m, \quad (37)$$

where v_i is the velocity on impact.

When results were computed, there was exact agreement between modeled results and Equations 34 through 37.

The next series of tests confirmed that individual model calculations were in exact agreement with hand-generated results. In this manner, each section of the computer program was tested and verified to have properly implemented the model equations when non-zero drag coefficients were used.

Tests were also conducted to evaluate the "reasonableness" of computer-modeled results. For example, checks were made to verify that the effects of wind on an aerial shell fired vertically are consistent with the shell's speed, i.e., are greatest just after the shell leaves the mortar, and then decrease until the shell reaches its apogee where the effects begin to increase again until the shell returns to the ground. The model successfully passed this series of tests.

The final and most definitive test was whether the model successfully reproduced results from field tests with real shells. This test also established that shell drift effects can be treated separately from ballistic results, i.e., that the problem is linear. The first set of results was for six-inch spherical shells. In this test, the mortar was angled to 24.5°, the azimuth was approximately south, and surface winds were ≤ 2 mph. Eight shells weighing an average of 39.4 ounces were fired. Their average flight time was 12.5 seconds and their average point-of-fall was 850 feet down range.

To determine the ballistic trajectory for these shells using the computer model, it was necessary to input a value for the shell's muzzle velocity. Average muzzle velocity was determined using the times of flight of the six-inch aerial shells fired previously when measuring shell drift effects. In this manner, an average muzzle velocity of 320 feet per second was established. Using this muzzle velocity and the measured average shell weight, the computer model predicted the average point of impact would be 825 feet down range. This level of agreement (within 3%) is exceptionally good considering the uncertainty in winds aloft and actual muzzle velocities.

When the distribution in the points of fall were considered, it was found that the average drift effect for shells propelled down range was 167 feet with a standard deviation of 113 feet. This is in

comparison with[4] 192 and 117-feet for the mean and standard deviation found in the previously reported study of spherical aerial shell drift effects. Considering the uncertainty in the reported results, the agreement between the two drift effect determinations is also exceptionally good.

Upon consideration of the above results and other similar tests, two conclusions were reached. The first is that the aerial shell ballistics problem is very nearly linear, and the other is that the model works well in predicting the average ballistic path of spherical aerial shells.

Sample Aerial Shell Ballistics Modeling Results

While it is not the purpose of this article to present an extensive series of modeled results, a few cases will be presented as examples of how the model can be of use.

One simple application of the model is the examination of trajectory parameters for spherical aerial shells for various mortar tilt angles. The modeled results to follow are for the conditions:

- Muzzle velocity = 320 feet per second,
- Shell diameter = 5.62 inches,
- Shell weight = 2.5 pounds,
- Wind speed = 0 miles per hour,
- Sea level drag coefficient = 0.36, and
- Elevation above sea level = 1,000 feet.

Figure 6 illustrates the ballistically predicted trajectories for shells fired from mortars with tilt angles of 5°, 25°, 55°, and 75° from vertical and azimuths of 0°. The various curves are plotted in the X–Z plane and thus form scaled representatives of the actual trajectories. The points shown on each curve are the locations of the shells for each second in time elapsed since firing. Thus, the distance between points is an indication of relative shell velocity. (Note, however, that in each case the final time interval just before impact is not a full second.)

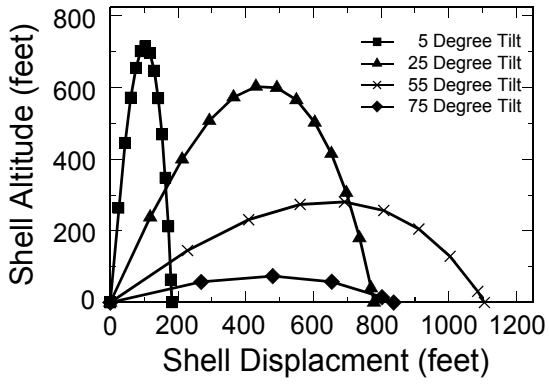

Figure 6. Ballistically predicted trajectories for shells fired from tilted mortars.

The curve for a 5° mortar tilt can be used to make a point about proper timing of bursts of aerial shells. Notice that the shell spends about four seconds traveling up and down only 70 feet about its apogee. Throughout this period of four seconds, the shell is traveling slowly, and the symmetry of its burst any time during this period would not be distorted by the shell's velocity. Some manufacturers feel that the optimum timing of a shell's burst is just after it reaches its apogee, which means the shell is already starting to come down. If the shell had lost some lift powder or there was a brief hang fire in the time fuse, such a shell could be dangerously close to the ground at the time of its burst. Obviously a more appropriate time (just as effective but safer) for the shell burst would be one (or even two) seconds before the shell reaches its apogee.

Figures 7 and 8 graphically present a collection of ballistic trajectory parameters for typical six-inch spherical aerial shells as a function of mortar tilt angle. Those parameters are apogee height, apogee displacement (the distance the shell has traveled down range at the time it reaches its apogee), impact point displacement (assuming the shell has not already burst), time to apogee, and time to impact. Besides demonstrating a capability of the modeling program, these graphs predict the effect of angled mortars on the location of normal shell bursts and the point where duds could fall. It is perhaps of some interest to note that the greatest impact point displacement is just over 1,100 feet (not considering drift effects) and occurs for a mortar tilt angle of approximately 53°, not at 45° as is often assumed. The reason for this is a result of drag force being proportional to velocity squared (see Equation 3), and the trajectory not being symmetric about the apogee.

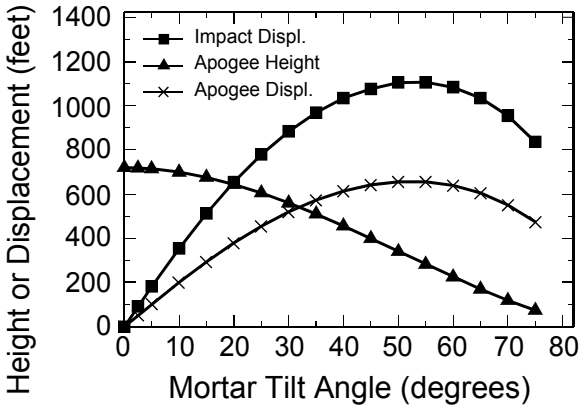

Figure 7. Ballistic trajectory parameters for 6" spherical aerial shells as a function of mortar tilt angle.

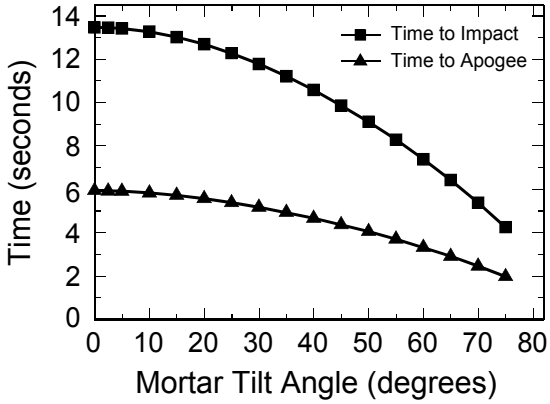

Figure 8. Ballistic trajectory parameters for 6" spherical aerial shells as a function of mortar tilt angle.

Another aspect of fireworks displays that is of considerable interest is the effect of wind on the trajectory of aerial shells and the debris created at the time of their bursts. Figure 9 graphs the displacement of typical six-inch spherical shells and their debris downwind as the result of varying wind conditions. Three sets of values are plotted; shell displacement at the time of apogee, shell displacement at the time of impact for a dud shell, and, for a normally functioning shell, debris displacement at the time the debris falls to the ground. In calculating the debris trajectory, after the shell reaches its apogee, new values for projectile mass, projected area, and drag coefficient are used by the computer-modeling program. Obviously, when a shell breaks the debris will have a great range of values for these three parameters, thus not all debris will fall at the same point. In addition, the debris will have a great range of velocities resulting from the exploding shell. Thus, the calculation of landing points for debris should be seen as only the very approximate center of the distribution. Nonetheless, it is instructive to consider the expected fallout point for debris, when examining the difficulty in performing a display in even moderate winds. In an attempt to be conservative with respect to the range of debris fallout, it was decided to track one of the most dense pieces of debris that would be expected. In these calculations the piece of debris has a mass equal to 3% of the shell, a projected area equal to 15% of the shell, and a drag coefficient equal to 3 times that of the shell. Figure 9 shows that the effects of wind on a shell's displacement at apogee are relatively minor; the effect on a dud shell's impact point is more significant; and the effect on a dense piece of debris is very substantial. (Note that while graphs in Figure 9 appear as straight lines, they are actually curving slightly.)

Information concerning the amount of mortar tilt needed to correct for the wind displacement effects is shown in Figure 10. The amount of mortar tilt indicated in Figure 10 for correction of shell apogee may be less than common experience might suggest. The reason for this is that the wind speed sensed by a display operator is the speed very near the ground. Because of obstructions to the wind (trees, buildings, people, etc.) the wind speed within five feet of the ground will usually be only a fraction of that above the obstructions. Perhaps a very crude rule of thumb is that the wind at chest height is only half of what it is at 50 feet. This underestimation of true wind speed

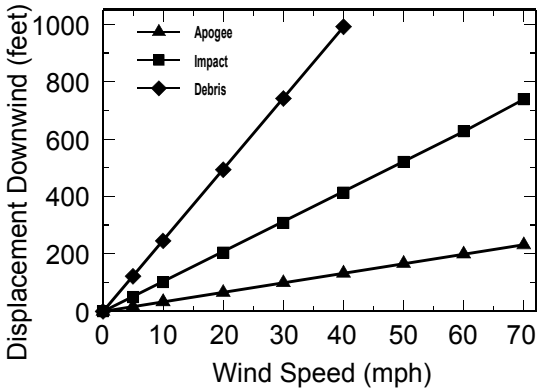

Figure 9. Displacement of 6" spherical aerial shell in wind.

makes it appear that the wind effect on a shell's displacement is somewhat greater than it actually is.

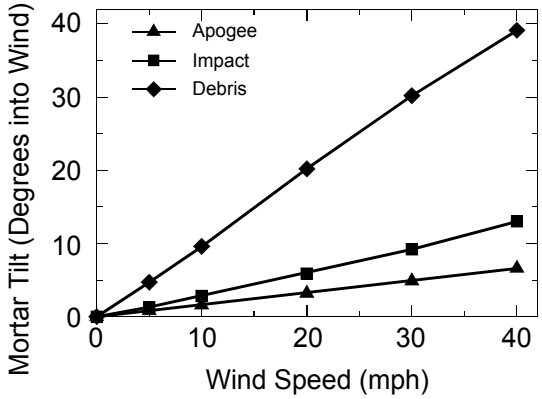

Figure 10. Amount of mortar tilt to correct for wind displacement.

The really important information in Figure 10 is that except for the trivial case of zero wind, there is no one mortar tilt angle that will completely correct for both the displacement of the a dud shell on impact and the point-of-fallout for dense debris. Figure 11 illustrates the ballistic trajectory for the case of a six-inch shell fired from a mortar tilted 6.6° into a 40 mph wind. This is the case where the mortar has sufficient tilt to compensate for the displacement of the shell's apogee. However, the tilt is significantly less than would be required to compensate for the drift in the landing point for a dud shell or for the debris from a properly functioning shell. Table 3 gives the required mortar tilts needed to compensate for the extreme case of a 40 mph wind.

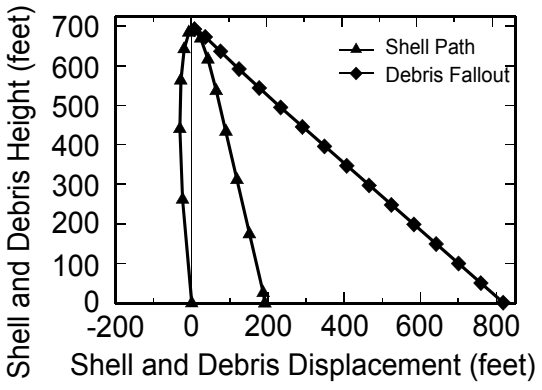

Figure 11. Ballistic trajectory of a 6" shell fired from a mortar tilted 6.6° into a 40 mph wind.

Table 3. Mortar Tilt Needed to Compensate for Effects of 40 mph Wind on a Typical 6" Spherical Shell.

Mortar Tilt Angle (degrees)	Displacement Down Wind (ft)		
	Shell at Apogee	Dud Shell at Impact	Debris Fallout
6.6	0	195	820
13.0	–115	0	650
39.1	–460	–590	0

From Table 3, it should be clear why it is not acceptable to fire a display in a 40 mph wind, unless spectators are kept at extremely great distances or are only upwind from the display. That is because, although it is possible to correct for any one of the displacements, the others can still present serious public safety concerns. A display can only be safely performed when the wind conditions are such that shells are not propelled toward spectators, and both duds and debris will fall safely within the secured area for the display.

Conclusion

The computer-modeling program presented in this article has been verified by both field experiment and analytical calculation. The modeling program has been used to generate some interesting and useful information that would have been too expensive to produce experimentally. The authors intend to continue their work and make further results available to the fireworks industry as they are completed.

Acknowledgments

The authors gratefully wish to acknowledge the technical and/or editorial suggestions made by E. Contestabile, T. Shimizu, R. Winokur, J. Bergman, and J. Taylor.

References

1) *Handbook of Physics*, Edited by E.V. Condon and H. Odishaw, McGraw Hill, NY, 1967.

2) *Van Nostrand's Scientific Encyclopedia,* Fifth edition. Van Nostrand, NY, *1976*.

3) K.L. and B.J. Kosanke, "Drift Effect for Spherical Aerial Shells," *Pyrotechnics Guild International Bulletin*, No. 74, 1991.

4) K.L. and B.J. Kosanke, "Statistical Distribution of Spherical Aerial Fireworks Shell Lateral Drift Effects," Presented at the *17th International Pyrotechnics Society Symposium*, Beijing, China, 1991.

5) T. Shimizu, *Fireworks from a Physical Standpoint*, Part 3, Table 35, Pyrotechnica Publications, Austin, TX, 1985.